



Cause and effect of N/P ratio decline with eutrophication aggravation in shallow lakes



Yao Zhang ^a, Chunlei Song ^{b,*}, Lei Ji ^c, Yuqian Liu ^d, Jian Xiao ^{b,e}, Xiuyun Cao ^b, Yiyong Zhou ^b

^a Center for Environment and Health in Water Source Area of South-to-North Water Diversion, School of Public Health and Management, Hubei University of Medicine, Shiyan 442000, PR China

^b Key Laboratory of Algal Biology, State Key Laboratory of Freshwater Ecology and Biotechnology, Institute of Hydrobiology, the Chinese Academy of Sciences, 7# Donghu South Road, Wuhan 430072, PR China

^c College of Life Science, Huaibei Normal University, Huaibei 235000, PR China

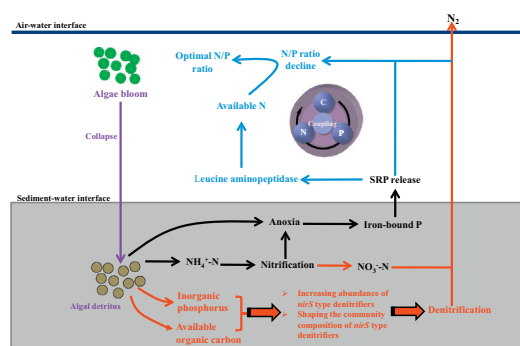
^d Yellow River Water Resources Protection Institution, Zhengzhou 450004, PR China

^e University of Chinese Academy of Sciences, Beijing 100039, PR China

HIGHLIGHTS

- The more eutrophic level, the lower N/P ratio
- P release from iron bound P and strong denitrification jointly caused low N/P.
- TOC and P fuelled PDR through regulating *nirS* denitrifiers.
- Low N/P caused LAP and GLU induction by high P, indicating nutrient coupling.

GRAPHICAL ABSTRACT



ARTICLE INFO

Article history:

Received 8 September 2017

Received in revised form 3 January 2018

Accepted 31 January 2018

Available online 7 February 2018

Editor: Ouyang Wei

Keywords:

N/P ratio

Denitrification

Phosphorus release

Eutrophication

Lake

ABSTRACT

To explore the relationship and cause and effect between eutrophication and the nitrogen (N)/phosphorus (P) ratio, samples from 38 lakes in Wuhan City, China, with differing degrees of eutrophication, were collected for nutrient levels and extracellular enzyme activities (EEA) in the water column from July 2011 to November 2011. The phosphorus fraction, abundance and potential denitrification rate (PDR) as well as community composition of *nirS*-type denitrifier in sediments of five typical lakes were further analyzed. A higher trophic level index (TSI) corresponded to a lower N/P ratio, which can be attributed to a loss of N and an increase in P. Specifically, in more eutrophic lakes, the enrichment of total organic carbon and all forms of P in sediments could fuel PDR by shaping community composition and increasing the abundance of *nirS*-type denitrifier as evidenced by correlation and redundancy analysis, ultimately resulting in a loss of N. Meanwhile, iron-bound phosphorus release induced by anoxia and the hydrolysis of organic P accounted for the observed increase of P in the water column. The lower N/P ratio facilitated the production of leucine aminopeptidase, which was unexpectedly induced by high P but not by low N. Similarly, alkaline phosphatase was induced by high N but not by low P. These findings indicate a mutual coupling and interplay between N and P cycling and confirm our hypothesis that P accumulation accelerates N loss in the process of eutrophication.

© 2018 Elsevier B.V. All rights reserved.

* Corresponding author.

E-mail addresses: clsong@ihb.ac.cn (C. Song), caoxy@ihb.ac.cn (X. Cao), zhouyy@ihb.ac.cn (Y. Zhou).

1. Introduction

Eutrophication is a world-wide environmental problem (Vollenweider, 1992), mainly caused by excessive input of N and P (Carpenter et al., 1998). The input of N and P to a certain extent changes the structure of water nutrition and the biological community (Chaffin et al., 2014). The coupling between N and P can affect the trophic webs and biogeochemical cycles of aquatic ecosystems (Yan et al., 2016) and is regulated by environmental factors and aquatic organisms (Sereda and Hudson, 2011).

N/P ratios play an important role in aquatic ecosystems, and are a significant component of the study of changes in trophic structure, biodiversity and biochemical cycles and have a strong influence on biological structure and function. The manipulation of N/P ratios is a widely used tool for managing phytoplankton species composition (Chislock et al., 2014). Previous studies have elucidated the close relationship between harmful algal blooms and the ratios of N/P (Peng et al., 2016). When eutrophication increases and the N/P ratio is low, cyanobacteria generally become dominant (Sondergaard et al., 2017; Isles et al., 2017). However, studies investigating the mechanism driving N/P ratio decline with eutrophication aggravation in shallow lakes generally focus on the imbalance of nutrient utilization by organisms and rarely focus on nutrient cycling processes of N and P.

The N cycle is comprised of multiple transformations of nitrogenous compounds, catalysed primarily by microbes (Zehr and Ward, 2002). Denitrification is recognized as the major nitrogen loss mechanism in many environments (Abed et al., 2013; Ward, 2013; Holmroos et al., 2012; Ginger et al., 2017). Denitrification is catalysed by four sequentially operating enzymes: nitrate reductase (Nar), nitrite reductase (Nir), nitric oxide reductase (Nor), and nitrous oxide reductase (Nos). Nitrite reductase (Nir), catalysing the reduction of NO_2^- to the gas NO , is considered the key enzyme of denitrification (Zumft, 1997; Kim et al., 2011). Functional marker genes such as the nitrite reductase gene *nirS* (short for cytochrome *cd1*-containing nitrite reductase), were targeted to study denitrifier communities. Understanding the composition of denitrifier communities could help us to better understand nitrogen cycling in lakes. The denitrifier community composition (Deslippe et al., 2014; Braker et al., 2015) and abundance (Wang et al., 2015; Zhou et al., 2016) can have a positive influence on PDR. Compared to oligotrophic lakes, the denitrification activities of eutrophic lakes are often more intense (Small et al., 2016), which contributes to a large proportion of N loss (Ginger et al., 2017). In addition, available P has been proven to have an important effect on the abundance and activity of denitrifiers (Tang et al., 2016). However, the effect of P on abundance, activity and community composition of denitrifier and the underlying mechanism for these effects has not been well documented.

Unlike the N cycle, the P cycle is internal (Lurling et al., 2016), and the sediment exchange of P determines the P level (Wu et al., 2017). The P in lake sediments is an inner nutrient source and can be released into overlying water to exacerbate algal blooms (Liu et al., 2016). In eutrophic lakes, this process can be strengthened by (Huang et al., 2016) anoxia, resulting in the release of iron-bound phosphorus from sediments (Li et al., 2016). Hence, we hypothesize that with eutrophication aggravation, the ratio of N/P in water should be correlated with N loss due to strong denitrification induced by P accumulation and P increase due to strong P release from sediments.

To explore whether the strengthened denitrification and P release resulted in the decline of N/P ratio with the aggressive of eutrophication and to test our hypothesis that P accumulation accelerates N loss in this process, we collected samples from 38 shallow lakes in Wuhan City to relate N and P concentrations and N/P ratios, and EEA with eutrophication levels. Five representative lakes or zones with different nutrient gradients were selected to study the phosphorus species in water and sediments, as well as the abundance, activity and community composition of *nirS*-type denitrifiers in sediments to identify the mechanism for N/P ratio mediated by denitrifier.

2. Materials and methods

2.1. Study sites and sample collection

In this study, in order to explore the relationship between eutrophication degree and N/P ratio in greater scale, samples from 38 lakes (some lakes were sampled in different sites) representing different nutrient concentration and different eutrophication level based on Li et al. (2016) were collected for nutrient level and EEA analysis in the water column from July 2011 to November 2011 in a subsection of Wuhan City (Fig. 1).

To further underline the relationship between N/P ratio and the eutrophication and better understand the reason from view of N loss through denitrification, five representative lakes or zones (5–6 replicates were taken from each lake, Lake Houguan: sampling site HG1–HG5, light-eutrophic, little macrophyte coverage; Lake Zhiyin: sampling site ZY1–ZY5, middle-eutrophic, aquaculture and algal bloom; East of Lake Tangxun: sampling site TX1–TX5, middle-eutrophic, aquaculture and anoxia; South of Lake Qingling: sampling site QL1–3, light-eutrophic, much macrophyte coverage; North of Lake Qingling: sampling site QL4–6, hyper-eutrophic, aquaculture and pollutant discharge) were chosen to sample again in June 2014. Additionally to water samples, in these five sites surface sediments (0–10 cm) samples were taken using a Peterson grab sampler to measure total organic matter (TOC), P fraction, PDR, abundance and community composition of *nirS*-type denitrifier.

All the samples were immediately stored in cooling boxes for transportation to the laboratory. The interstitial water was separated from the sediment particles by centrifugation at 3000 rpm for 20 min (Degobbis et al., 1986). The supernatants and water samples were then filtered through a 0.45 μm membrane filter for analysis of soluble nutrients. The sediments were stored at 4 °C in the dark for two to four days before analysis.

2.2. Nutrient analysis of water and sediment samples

All the nutrient measurements in water samples, including ammonium (NH_4^+ -N), nitrite (NO_2^- -N), nitrate (NO_3^- -N), dissolved total nitrogen (DTN), total nitrogen (TN), soluble reactive phosphorus (SRP), dissolved total phosphorus (DTP) and TP, followed national standards (APHA, 2012). The dissolved inorganic nitrogen (DIN) was calculated as the sum of NH_4^+ -N, NO_2^- -N and NO_3^- -N. TSI was calculated using three limnological parameters including Chl *a* ($\mu\text{g L}^{-1}$), Secchi disk transparency (Trans) (m) and TP ($\mu\text{g L}^{-1}$) according to Carlson (1977), which can be referred to Li et al. (2016). Sediment P fractionation was carried out according to Golterman (1996). This method groups sediment P into Fe(OOH)-P, calcium-bound P (CaCO_3 -P), acid-soluble organic P (ASOP) and hot NaOH-extractable organic P (P_{alk}). Sediment total organic carbon (TOC) was determined by TOC Analyzer (Analytikjena HT1300).

2.3. Analysis of EEA

EEA, including alkaline phosphatase activity (APA) and leucine aminopeptidase activity (LAP), were determined according to Hoppe (1983). Briefly, triplicates of 2.7 ml subsamples were supplied with Tris-HCl buffer (pH = 8.5, final concentration 5.2 mmol L^{-1}) and incubated separately with a 100 μM concentration of each specific fluorogenic substrate analogues L-leucine-4-methylcoumarinylamid hydrochloride and 4-methylumbelliferyl phosphate (Sigma). The fluorescence released by substrate hydrolysis was measured with a Sanco 960 spectrofluorometer as the increase between 0 time (initial time) and 2–3 hour incubation at the “in situ” temperature. Calibration curves with concentrations from 200 to 800 nM of 7-amino-4-methylcoumarin (MCA) and 4-methylumbelliferone (MUF) were performed for LAP and APA, respectively. Data are expressed in terms of the potential

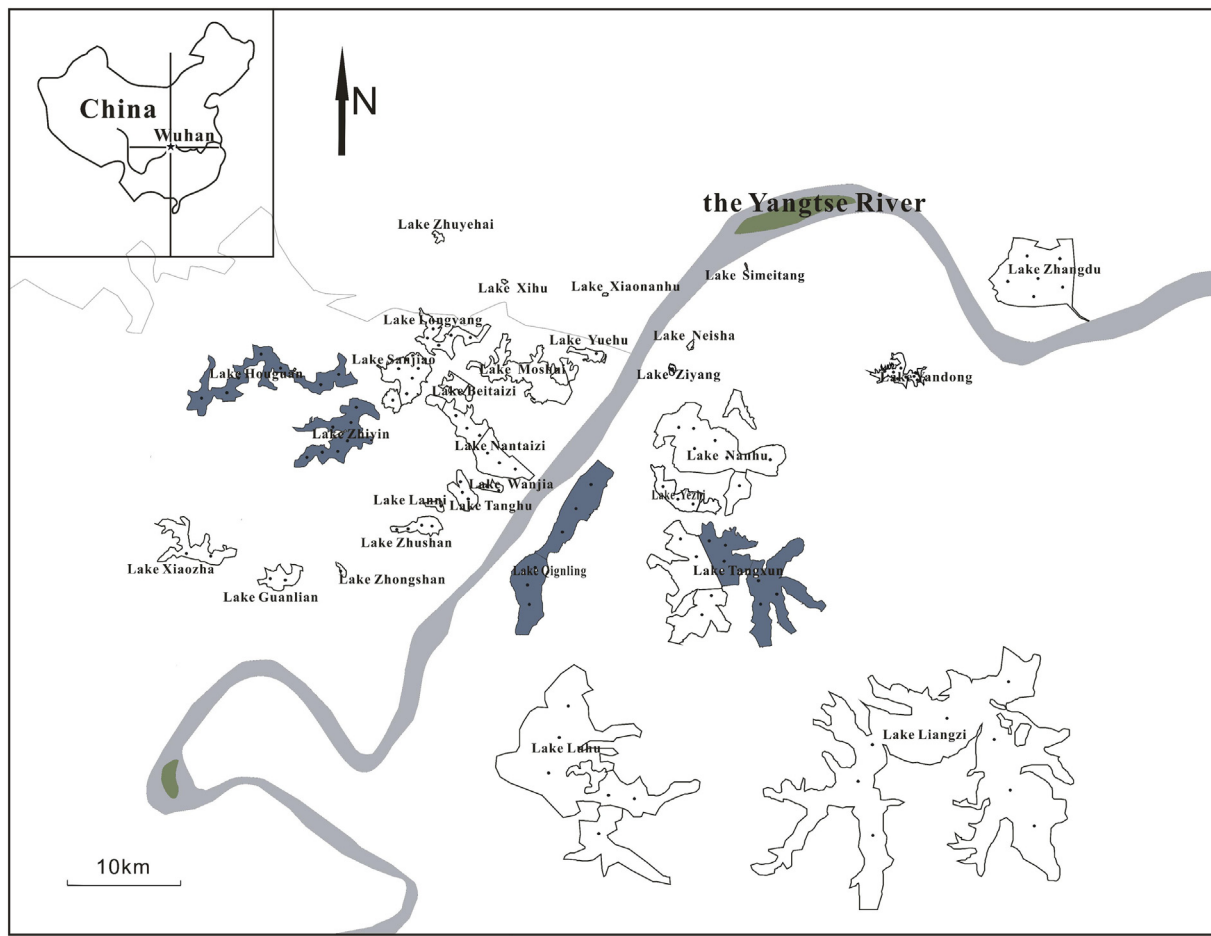


Fig. 1. The distribution map of all studied sites in Wuhan City (blue lakes represent the sites selected to perform the study of PDR and *nirS* community composition in sediments). (For interpretation of the references to color in this figure legend, the reader is referred to the web version of this article.)

hydrolysis rate of the substrates, as $\mu\text{g N}$ and $\mu\text{g P}$ potentially released per hour, respectively.

2.4. Determination of potential denitrification rate (PDR) of sediment

The sediment PDR was measured based on the Denitrifying Enzyme Activity (DEA) Assay (Jha and Minagawa, 2013). Briefly, 5 g of sediment was placed in a custom-made borosilicate glass bottle with 20 ml of DEA solution (7 mM of KNO_3 , 3 mM of glucose and 5 mM of chloramphenicol). Oxygen was purged from each bottle by continuously pumping helium and acetylene was added to reach a final concentration of 10%. Sample bottles were placed on an orbital shaker and shaken (125 r/min) in the dark at 25 °C. Gas samples were taken at 0, 0.5, 1, 1.5 and 2 h for N_2O measurement using a gas chromatograph. The PDR was calculated as the slope of the best fit curve of the N_2O concentration as a function of time.

2.5. Abundance and community composition of *nirS*-type denitrifier

DNA was extracted from approximately 0.3 g fresh sediment samples by UltraClean Soil DNA Isolation Kit (Mo Bio Laboratories, Carlsbad, CA) according to the manufacturer's instructions. Quantitative polymerase chain reaction (qPCR) assays were performed using the primers *nirS1F* (CCT AYT GGC CGG CRC ART) and *nirS3R* (GCC GCC GTC RTG VAG GAA) (Levy-Booth and Winder, 2010). Reactions were performed with 10 ng template DNA and 0.1 μM concentrations of each primer in a total volume of 20 μl . The cycling conditions were: 95 °C for 30 s, 30 cycles of 5 s at 95 °C, 30 s at 57 °C, 40 s at 72 °C, and 7 min at 72 °C.

Denitrifier (*nirS*) community composition was analyzed via terminal restriction fragment length polymorphism (T-RFLP) targeting the cytochrome *cd1* nitrite reductase gene. The forward primer was fluorescently labelled at the 5' end with 6-carboxyfluorescein (FAM). Polymerase chain reaction (PCR) amplifications of *nirS* genes from total environmental DNA extracts were performed with primers FAM-*nirS1F* and *nirS6R* using conditions described previously (Braker et al., 2000; Braker et al., 2001). After purification, approximately 10 ng of *nirS* PCR products were digested for 3 h at 37 °C with the *HhaI* and *RsaI* and at 65 °C with *TaqI* restriction enzyme (MBI Fermentas, Hanover, MD). After digestion, 2 μl of each sample was mixed with 12 μl of formamide and 0.3 μl of LIZ-labelled internal size standard. Fragment size analysis was carried out with the ABIPRISM 3730xl genetic analyzer. The peak heights were automatically quantified by GENESCAN analysis software (Applied Biosystems). Given the differences in run time among all samples, we considered fragments from different profiles with <1 bp difference to be the same.

2.6. Statistical analysis

Pearson's test was performed using the SPSS 18.0 package (SPSS, Chicago, IL) with a value of 0.05 or 0.01 selected for significance analysis of parameters between N, P or N/P and TSI in lakes of Wuhan City, PDR, abundance, community composition of *nirS*-type denitrifiers and environmental parameters in five typical lakes or zones to explore the correlation between them. Microbial community profiles were statistically analyzed for differences in T-RFLP results using analysis of similarity. Non-metric multidimensional scaling (NMDS) map was used to show

Table 1
Comparison of different inorganic nutrient forms, extracellular enzymes activities (EEA) and TSI in all studied lakes.

Lake name (n)	SRP	DTP	TP	NO ₃ ⁻ -N	NO ₂ ⁻ -N	NH ₄ ⁺ -N	TSI ^a	APA	LAP
Lake Nanhu (7)	353.93 ± 50.12	407.15 ± 52.89	620.22 ± 48.04	3514.96 ± 184.41	4695.42 ± 416.84	959.36 ± 615.44	80.89 ± 1.18	29.99 ± 5.09	3.51 ± 0.53
Lake Yezhi (3)	156.92 ± 62.04	166.64 ± 73.65	580.67 ± 125.43	167.06 ± 124.52	204.45 ± 117.01	74.69 ± 42.61	82.62 ± 1.75	40.07 ± 4.36	2.51 ± 0.30
Lake Qingling (N, 3)	760.58 ± 363.18	798.85 ± 430.70	1493.25 ± 77.13	27.99 ± 8.36	24.36 ± 2.81	340.30 ± 201.73	83.54 ± 4.11	2.91 ± 0.21	4.42 ± 0.89
Lake Qingling (S, 3)	13.18 ± 4.57	30.36 ± 12.57	151.19 ± 142.24	20.19 ± 7.80	23.11 ± 18.55	133.95 ± 6.94	70.28 ± 2.76	3.04 ± 0.14	1.59 ± 0.11
Lake Yehu (1)	12.60	22.35	323.71	0	15.61	489.26	82.83	3.63	4.37
Lake Huangjia (1)	62.54	78.70	333.21	12.39	11.86	119.03	80.28	3.39	4.12
Lake Yandong (7)	8.76 ± 0.99	15.47 ± 4.59	55.55 ± 25.06	1.99 ± 0	11.86 ± 3.56	7.67 ± 5.60	56.14 ± 8.73	3.92 ± 0.68	0.66 ± 0.27
Lake Yangchun (1)	7.95	18.05	53.06	85.18	0	617.69	56.57	0.37	0.14
Lake Ziyang (2)	524.13 ± 152.61	534.97 ± 203.46	853.91 ± 60.32	2.60 ± 0.61	0	0	71.68 ± 3.39	0	1.68 ± 0.87
Lake Neisha (1)	20.33	33.33	144.10	53.98	0	889.36	68.33	0.89	0.88
Lake Simeitang (2)	30.05 ± 2.06	40.65 ± 0.45	86.80 ± 4.50	0	0	0	56.76 ± 0.01	1.98 ± 0.09	1.21 ± 0.58
Lake Shaihu (2)	612.22 ± 70.41	967.33 ± 278.34	1682.56 ± 147.35	150.16 ± 23.40	0	1818.39 ± 80.35	82.97 ± 2.80	0.71 ± 0.04	3.45 ± 0.09
Lake Tangxun (10)	27.85 ± 27.85	77.36 ± 75.43	250.70 ± 115.01	134.57 ± 103.40	102.80 ± 87.99	635.44 ± 415.27	70.58 ± 3.16	0.88 ± 0.32	1.73 ± 0.26
Lake Jiqidang (1)	10.64	23.39	128.64	480.29	611.38	791.73	69.91	1.08	1.34
Lake Xihu (1)	21.06	22.73	109.44	163.16	25.40	500.40	60.29	0.94	0.59
Lake Houxianghe (1)	12.96	23.39	155.12	173.56	81.88	1335.67	63.90	2.42	0.56
Lake Lingjiao (1)	41.31	50.53	311.34	100.77	0	791.73	81.56	1.06	4.11
Lake Tazi (1)	267.50	280.89	439.77	90.37	0	0	75.04	0.77	1.51
Lake Zhuyehai (1)	18.74	41.92	284.87	116.37	0	286.54	79.00	0.68	2.85
Lake Xiaonanhu (1)	12.96	18.09	175.64	95.57	5.98	1050.53	70.83	0.46	0.88
Lake Nantaizi (6)	129.13 ± 41.21	155.89 ± 44.41	346.11 ± 34.39	250.67 ± 40.87	288.67 ± 49.92	2099.91 ± 540.46	74.39 ± 1.27	0.29 ± 0.07	0.78 ± 0.13
Lake Beitaizi (3)	30.33 ± 10.62	56.14 ± 12.93	203.15 ± 13.37	133.27 ± 20.26	7.61 ± 5.72	986.31 ± 405.41	70.88 ± 1.13	0.66 ± 0.09	0.97 ± 0.08
Lake Sanjiao (5)	113.21 ± 42.43	134.78 ± 38.71	147.39 ± 52.49	266.10 ± 27.10	271.46 ± 125.61	941.99 ± 481.17	76.76 ± 2.90	1.25 ± 0.07	2.39 ± 0.27
Lake Longyang (5)	180.33 ± 76.02	413.97 ± 59.41	1080.33 ± 84.99	608.19 ± 383.11	2063.99 ± 232.47	4676.02 ± 1496.05	82.41 ± 1.40	1.76 ± 0.70	1.75 ± 0.52
Lake Tanghu (3)	33.05 ± 3.99	43.51 ± 19.18	351.44 ± 54.47	90.37 ± 33.69	0	768.10 ± 412.87	74.20 ± 0.76	0.87 ± 0.15	1.66 ± 0.31
Lake Wanjia (2)	390.79 ± 6.59	431.75 ± 7.75	619.48 ± 3.19	77.38 ± 12.80	81.75 ± 14.29	851.71 ± 147.35	72.76 ± 0.23	0.72 ± 0.01	1.42 ± 0.30
Lake Zhiyin (7)	9.34 ± 4.98	23.41 ± 8.50	124.26 ± 23.94	147.56 ± 107.52	100.51 ± 29.55	1208.80 ± 157.75	67.27 ± 1.26	11.07 ± 0.23	1.36 ± 0.26
Lake Houguan (7)	8.79 ± 2.58	19.97 ± 4.91	51.02 ± 14.07	147.56 ± 34.37	33.91 ± 21.33	49.02 ± 34.37	55.59 ± 4.14	17.23 ± 0.94	0.41 ± 0.08
Lake Gaohu (5)	8.32 ± 0.78	21.21 ± 2.58	207.61 ± 15.14	89.33 ± 82.88	30.54 ± 28.96	1514.24 ± 840.86	78.65 ± 0.53	16.72 ± 0.66	1.59 ± 0.10
Lake Zhushan (4)	101.02 ± 17.38	208.57 ± 45.54	299.95 ± 18.64	281.43 ± 66.92	373.59 ± 38.52	886.19 ± 588.41	76.49 ± 1.58	20.35 ± 2.15	1.17 ± 0.16
Lake Lanni (1)	106.42	244.10	272.52	974.19	1278.60	2575.96	69.95	21.90	0.82
Lake Zhongshan (1)	63.83	158.17	227.58	397.11	0	650.28	66.95	19.94	0.97
Lake Guanlian (2)	237.64 ± 89.55	338.95 ± 175.27	543.53 ± 176.67	641.45 ± 208.27	0	1576.67 ± 352.57	-	1.61 ± 0.93	1.65 ± 0.06
Lake Xiaozha (2)	5.73 ± 1.72	10.44 ± 4.21	94.72 ± 7.48	27.98 ± 6.53	0	1306.28	74.01 ± 0.43	1.11 ± 0.09	2.09 ± 0.02
Lake Liangzi (8)	6.16 ± 4.38	10.42 ± 5.68	63.50 ± 8.50	100.45 ± 31.81	0	49.24 ± 14.15	62.62 ± 2.35	2.75 ± 0.25	0.43 ± 0.08
Lake Zhangdu (6)	7.10 ± 1.64	10.21 ± 0.72	73.92 ± 16.42	65.24 ± 34.67	0	92.40 ± 37.69	61.05 ± 3.68	2.28 ± 0.05	0.34 ± 0.05
Lake Daoshuihe (1)	7.31	16.38	189.89	584.27	0	0	-	2.49	0.46
Lake Luhu (6)	-	8.73 ± 4.56	14.35 ± 2.22	-	-	-	-	4.56 ± 0.30	0.86 ± 0.07

"0": below detection limit; "-": no data, n means sampling sites numbers of each lake.

Unit: µg L⁻¹ for NO₃⁻-N, NO₂⁻-N, NH₄⁺-N, SRP, TN; APA: alkaline phosphatase activity, µg P L⁻¹ h⁻¹; LAP: leucine aminopeptidase activity, µg C L⁻¹ h⁻¹; TSI: trophic state index, calculating by Chl *a* (µg L⁻¹), Trans (m) and TP (µg L⁻¹).

^a TSI and TP value was cited from Li et al. (2016).

Table 2
Pearson's correlation coefficients between EEA, TSI and nutrient forms in water column of studied lakes.

	SRP	DTP	TP	NO ₃ ⁻ -N	NO ₂ ⁻ -N	NH ₄ ⁺ -N	DIN	DTN	TN
APA	-0.049	-0.025	-0.065	0.265**	0.111	-0.176	0.015	-0.008	0.149
LAP	0.539**	0.597**	0.683**	0.204*	0.173	0.218*	0.186	0.292**	0.524**
TSI ^a	0.420**	0.434**	0.589**	0.277**	0.321**	0.395**	0.206	0.446**	0.468**

APA: alkaline phosphatase activity; LAP: leucine aminopeptidase activity.

TSI: trophic state index, calculating by Chl *a* (μg L⁻¹), Trans (m) and TP (μg L⁻¹).

** Significance at α = 0.01 level.

* Significance at α = 0.05 level.

^a TSI and TP value was cited from Li et al. (2016).

the distribution of *nirS*-type community composition, and then added the PDR as symbols in it to show the relationship between *nirS*-type community and PDR, which was analyzed with RELATE modular. The location of sampling sites represented the community structure and the size of the bubble value represents different PDR (Primer V 5.0 software, PRIMER-E, Plymouth, UK). Redundancy analysis (RDA) was used to identify the key factors regulating the community structure of *nirS*-type denitrifiers with the software CANOCO for Windows, version 4.5 (Ter Braak and Šmilauer, 2002).

3. Results

3.1. Relationships among nutrient species, N/P, EEA and TSI

Mean values of TSI, nutrient levels and EEA for each lake are described in Table 1. Almost all N forms (NO₃⁻-N, NO₂⁻-N, NH₄⁺-N, DTN and TN) and P forms (SRP, DTP and TP) were significantly and positively correlated with TSI (Table 2), while their ratios (TN/TP, DTN/DTP, NH₄⁺-N/SRP, NO₃⁻-N/SRP, NO₂⁻-N/SRP, DTN/SRP, and DIN/SRP) showed a significantly negative correlation with TSI in all studied lakes (Table 3 and Fig. 2). Notably, the ratio of DIN to TN showed a significantly negative correlation with TSI ($r = -0.207$, $P < 0.01$, Fig. 2), although DIN and TN were not used to calculating TSI. LAP was significantly and positively correlated with SRP, DTP, TP and TN ($P < 0.01$, Table 2). APA showed a significantly positive relationship with TN ($P < 0.01$, Table 2).

3.2. Relationships between PDR, TSI and *nirS*-type denitrifiers

PDR exhibited a more significantly positive relationship with *nirS* copy numbers ($r = 0.550$, $P < 0.01$, Fig. 3) than TSI ($r = 0.413$, $P < 0.01$, Fig. 3), and also a significantly negative correlation with N/P ratio (TN/TP, DTN/DTP, NH₄⁺-N/SRP, NO₃⁻-N/SRP, NO₂⁻-N/SRP, DTN/SRP and DIN/SRP) (Table 3). RELATE analysis showed that the more similar the PDR values are, the more similar the community composition of *nirS*-type denitrifiers ($P < 0.05$, Fig. 4). NMDS analysis showed that community composition of *nirS*-type denitrifiers of the same lake (basin) had high T-RF similarity and were clustered together (Fig. 4).

3.3. Relationships between environmental factors and *nirS*-type denitrifier

The copy number of *nirS* exhibited a significantly positive relationship with concentration of SRP in interstitial water ($r = 0.590$, $P < 0.01$), Fe

(OOH)—P ($r = 0.610$, $P < 0.01$) and CaCO₃—P ($r = 0.539$, $P < 0.05$) in sediments of five studied sites (Table 4). Community structure of *nirS*-type denitrifiers showed a significant correlation with the concentration of different phosphorus forms (SRP, DTP, TP and SRP_i) in water ($P < 0.01$) and all fractions of phosphorus (Fe(OOH)—P, CaCO₃—P, ASOP and P_{alk}) ($P < 0.01$) in sediments (Table 4).

The eigenvalues of the first and the second axes were 0.476 and 0.313, respectively. The cumulative percentage variance of the species-environment relationship was 52.4% for the first axis and 86.8% for the two axes (Fig. 5). The first axis was mainly regulated by Fe (OOH)—P, NH₄⁺_{int}, TOC and TN with correlation coefficients of 0.5964, 0.5990, 0.4878 and 0.4411, respectively. The second axis was mainly regulated by SRP, DTP, TP and PDR with correlation coefficients of 0.9322, 0.9031, 0.9006 and 0.8627, respectively.

4. Discussion

The studied lakes represent different degrees of eutrophication based on the TSI (Table 1), reflecting the lakes diversity. With the TSI increase, the increase of N and P concentration was expected, what is more interesting is the decline of N/P ratios (Tables 2, 3 and Fig. 2). This indicates that the increased stock amount of N in the water column was far below that of P with eutrophication aggravation. This phenomenon has been observed in many cases (Cunha et al., 2013; Han et al., 2014), which can be attributed to the loss of N and/or release of P.

Denitrification is mainly responsible for the loss of N in eutrophic lakes (Ward, 2013). In this study, the significantly positive relationship between the TSI and PDR and abundance of *nirS*-type denitrifiers (Fig. 3, Table 4) suggests that eutrophication aggravation stimulated the growth and function of *nirS*-type denitrifiers, which directly resulted in the loss of N. This was further proven by the significantly negative correlation between PDR and N/P ratio (Table 3). Hence, higher PDR in more eutrophic lakes is an important cause of N loss and low N/P ratio.

NMDS and correlation analysis indicated that PDR was closely related to the abundance and community composition of *nirS*-type denitrifiers (Fig. 4 and Table 4). The shift in the denitrifier community structure with higher rates of N removal via denitrification suggests that microbial community structure may influence biogeochemical processes (Tatariw et al., 2013). The increase of PDR was mirrored by the shift in *nirS* denitrifier community composition (Yin et al., 2015). In this study, high similarity of *nirS*-type denitrifiers community composition within the same lake (Fig. 4) illustrated that there was a unique

Table 3
Pearson's correlation coefficients describing the relationships between the TSI, PDR and ratio of nitrogen to phosphorus in all studied lakes.

	TN/TP ^a	DTN/DTP	NH ₄ ⁺ -N/SRP	NO ₃ ⁻ -N/SRP	NO ₂ ⁻ -N/SRP	DIN/SRP	DIN/TP ^a
TSI ^a	-0.275**	-0.225**	-0.291**	-0.404**	-0.352**	-0.545**	-0.311**
PDR	-0.360**	-0.150	-0.339*	-0.334*	-0.263	-0.331**	-0.543**

PDR: potential denitrification rate.

TSI: trophic state index, calculating by Chl *a* (μg L⁻¹), Trans (m) and TP (μg L⁻¹).

** Significance at α = 0.01 level.

* Significance at α = 0.05 level.

^a TSI and TP value was cited from Li et al. (2016).

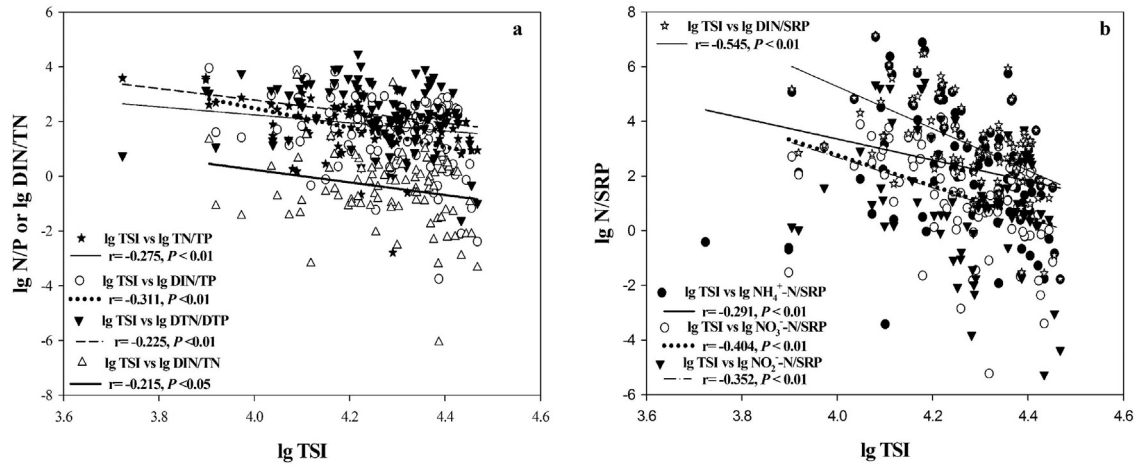


Fig. 2. Scatter plots of the correlations between TSI and N/P, DIN/TN (a) and N/SRP (b) in the water column of all the studied sites. TSI: trophic state index, calculating by Chl *a* ($\mu\text{g L}^{-1}$), Trans (m) and TP ($\mu\text{g L}^{-1}$). TSI and TP values were cited from Li et al. (2016).

community composition of the *nirS*-type denitrifiers in each lake, which might directly influence the PDR. Hence, the abundance and community composition of the *nirS*-type denitrifiers could determine the degree of PDR.

Additionally, in this study, the *nirS*-type denitrifier community composition was mainly regulated by different P forms and TOC, as illustrated by the significant relationship between the *nirS*-type denitrifier community composition and SRP, DTP, and TP in the water column, SRP in interstitial water, all P fractions and TOC in sediment (Table 4). This fact was further proven by RDA analysis (Fig. 5). The abundance of *nirS*-type denitrifier had a close relationship with SRP in interstitial water as well as Fe(OOH)—P in sediments. Additionally, PDR may be influenced by TP in the water column and by all P fractions in sediments (Table 4). This evidence suggests a close coupling between denitrifiers and C and P, but not N. In Swedish boreal lake sediments, enhanced C and P availability likely promoted the PDR (Myrstener et al., 2016). RDA analysis showed that water content and available phosphorus in wetland sediment served as the driving factor in shaping the *nirS* denitrifying bacterial community (Gu et al., 2017). However, the correlation between *nirS*-type denitrifiers and nitrate in the sediment of Lake Baiyangdian was not significant (Wang et al., 2017). Thus, it can be deduced that compared to N, the enrichment of P and C in the

eutrophication process could fuel PDR more by shaping community composition and increasing the abundance of denitrifiers, ultimately resulting in a loss of N.

Nutrient enrichment in eutrophic lakes usually caused an algal bloom, which would settle upon the surface sediment as organic matter following the bloom. The decomposition of organic matter not only produced a great amount of inorganic phosphorus, NH_4^+ -N and available organic carbon, but also led to anoxia in sediments (Li et al., 2016). The accumulation of NH_4^+ -N further accelerated the anoxic formation through nitrification (Clevinger et al., 2014). Anoxia is often found in eutrophic water bodies, which stimulates P release from Fe(OOH)—P (Muller et al., 2016). In addition, higher CaCO_3 —P and ASOP in eutrophic lakes, as evidenced by the positive relationship between CaCO_3 —P, ASOP and PDR (Table 4), should be considered important P release pathways through inorganic and organic phosphorus-solubilizing bacteria (Song et al., 2009; Liu et al., 2017). Taken together, in eutrophic lakes, the N loss and P release jointly resulted in the low N/P ratio.

A low N/P ratio can have an important effect on the activity and community composition of algae and microbes in the water column. For all organisms, there is an optimal balance of nutrients, and importantly, both above and below this optimum, there is a metabolic cost, and

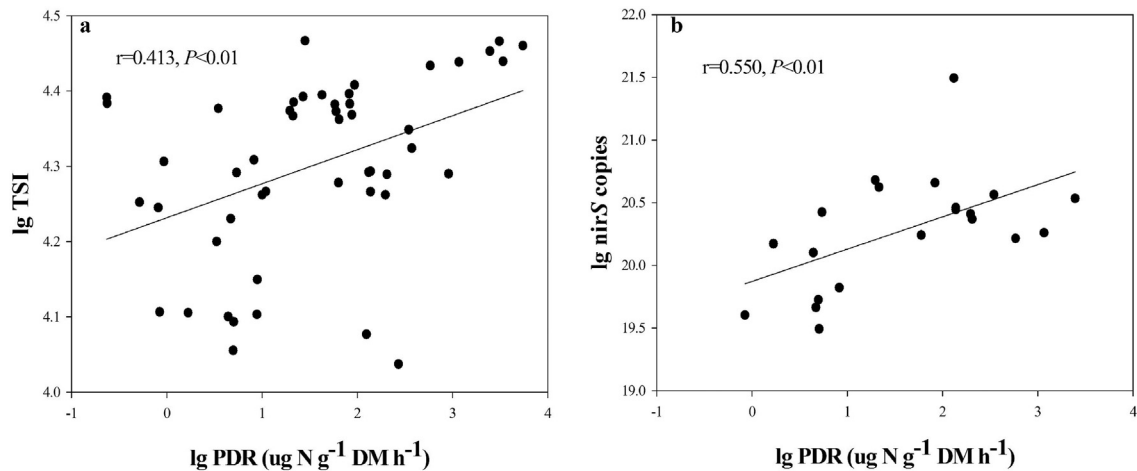


Fig. 3. Scatter plots of the correlations between PDR and TSI (a) and abundance of *nirS*-type denitrifiers (b) in the five studied sites. PDR: potential denitrification rate. TSI: trophic state index, calculating by Chl *a* ($\mu\text{g L}^{-1}$), Trans (m) and TP ($\mu\text{g L}^{-1}$).

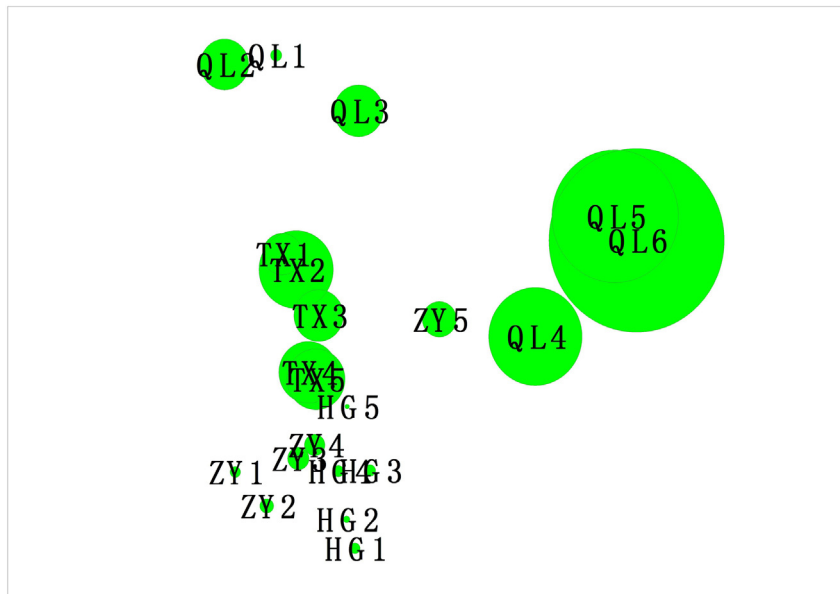


Fig. 4. NMDS analysis of *nirS*-type denitrifier community composition and RELATE analysis of *nirS*-type denitrifier community composition and PDR in sediments of the five studied sites. The letters mean site names, the location of letters (center of the circle) represents the community structure similarity and the size of the bubble represents PDR value.

there can be potential compensatory mechanisms (Glibert, 1998). In this study, the significantly positive relationship between LAP and P (SRP, DTP, TP) (Table 2) suggested that P enrichment in eutrophic lakes activated the LAP to compensate for the relative deficiency of available N. Likewise, APA was induced by TN as evidenced by their positive relationship (Table 2). Notably, in this study, EEA could be induced by non-substrate nutrients with high concentrations but not by usual substrate nutrients with low concentrations, indicating the broader complexity and relevancy among different nutrients (Glibert, 2017). Hence, the effect of the N/P ratio imbalance was the self-regulation of ecosystems through the mediation of nutrient regeneration and utilization at scales ranging from physiological to ecological.

5. Conclusions

In shallow lakes, the more eutrophic they are, the lower the N/P ratio. The major driver of this phenomenon is N loss through denitrification and P increase through the release of Fe(OOH)—P, CaCO₃—P and ASOP. Specifically, in lakes that are more eutrophic, the enrichment of TOC (algal detritus settlement) and all forms of P in sediments could fuel PDR by shaping community composition and increasing the abundance of the *nirS*-type denitrifier, ultimately resulting in a loss of N.

The increase in P can be attributed to the release of Fe(OOH)—P mediated by anoxic status and the hydrolysis of CaCO₃—P and ASOP by microbes. The lower N/P ratio affected the production of extracellular enzymes to compensate for the relative deficiency of nutrients. Interestingly, LAP was induced by high P, but not low N. Similarly, APA was induced by high N, but not low P. These findings indicate a mutual coupling and interplay between N and P cycling, especially in eutrophic lakes.

Acknowledgement

This work was supported by grants from the National Key Research & Development Program of China (2016YFE0202100), the National Natural Science Foundation of China (41230748; 41573110; 41706136; 81372998), the Major Science and Technology Program for Water Pollution Control and Treatment (2017ZX07603), the State Key Laboratory of Freshwater Ecology and Biotechnology (2016FBZ07), Anhui Provincial Natural Science Foundation (1708085QC71), key projects of Anhui province university of outstanding youth talent support program (GXGNFX2018010), the Foundation for Innovative Research Team of Hubei University of Medicine (FDFR201602) and a Faculty Development Grant from Hubei University of Medicine (2016QDJZR16).

Table 4

Pearson's correlation coefficients describing the relationship between PDR, abundance, community composition of *nirS* type denitrifiers and environmental parameters in five typical lakes or zones.

	TSI*	SRP	DTP	TP	NH ₄	NO ₃	NO ₂	DTN	TN	SRPi	NH ₄ i	NO ₃ i	NO ₂ i	FeP	CaP	ASOP	P _{alk}
AND	0.560**	0.319	0.198	0.370	0.201	0.254	-0.046	0.405	0.540*	0.590**	0.401	0.639**	0.088	0.610**	0.539*	0.400	0.421
CCND	0.198*	0.473**	0.294**	0.36**	0.205	0.076	0.372**	-0.013	0.145*	0.331**	0.431**	0.121	0.115	0.507**	0.562**	0.718**	0.654**
PDR	0.755**	0.548*	0.357	0.652**	0.180	0.312	-0.045	0.577**	0.785**	0.499*	0.776**	0.636**	0.256	0.593**	0.890**	0.764**	0.628**

NH₄: NH₄⁺-N in water column; NO₃: NO₃⁻-N in water column; NO₂: NO₂⁻-N in water column; SRPi: SRP in interstitial water; NH₄i: NH₄⁺-N in interstitial water; NO₃i: NO₃⁻-N in interstitial water; NO₂i: NO₂⁻-N in interstitial water; TOC: total organic carbon in sediments; FeP: Fe(OOH)—P; CaP: CaCO₃—P; ASOP: acid-soluble organic phosphorus; P_{alk}: NaOH-extractable organic phosphorus.

AND: abundance of *nirS*-type denitrifier.

CCND: community composition of *nirS*-type denitrifier.

PDR: potential denitrification rate.

TSI: trophic state index, calculating by Chl *a* (μg L⁻¹), Trans (m) and TP (μg L⁻¹).

** Significance at α = 0.01 level.

* Significance at α = 0.05 level.

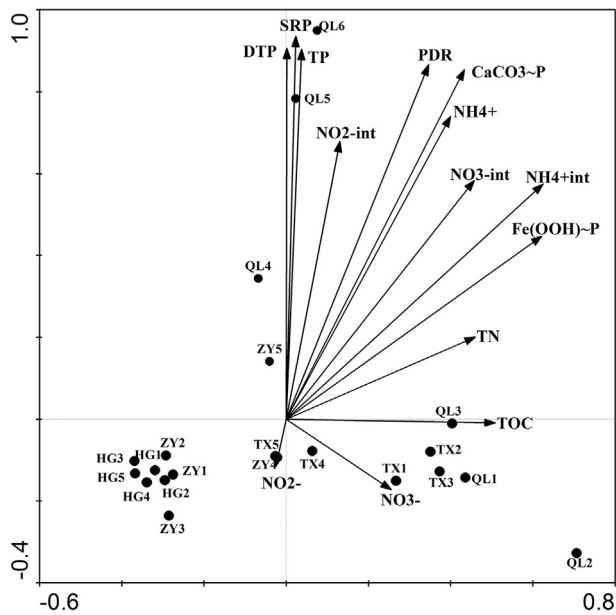


Fig. 5. Redundancy analysis (RDA) based on *nirs* T-RFLP patterns and environmental parameters in the five studied sites. TSI: trophic state index, calculating by Chl *a* ($\mu\text{g L}^{-1}$), Trans (m) and TP ($\mu\text{g L}^{-1}$). PDR: potential denitrification rate.

References

- Abed, R.M.M., Lam, P., de Beer, D., Stief, P., 2013. High rates of denitrification and nitrous oxide emission in arid biological soil crusts from the Sultanate of Oman. *ISME J.* 7 (9): 1862–1875. <https://doi.org/10.1038/ismej.2013.55>.
- Braker, G., Zhou, J.Z., Wu, L.Y., Devol, A.H., Tiedje, J.M., 2000. Nitrite reductase genes (*nirK* and *nirS*) as functional markers to investigate diversity of denitrifying bacteria in Pacific northwest marine sediment communities. *Appl. Environ. Microbiol.* 66 (5): 2096–2104. <https://doi.org/10.1128/AEM.66.5.2096-2104.2000>.
- Braker, G., Ayala-del-Río, H.L., Devol, A.H., Fesefeldt, A., Tiedje, J.M., 2001. Community structure of denitrifiers, bacteria, and archaea along redox gradients in Pacific Northwest marine sediments by terminal restriction fragment length polymorphism analysis of amplified nitrite reductase (*nirS*) and 16S rRNA genes. *Appl. Environ. Microbiol.* 67:1893–1901. <https://doi.org/10.1128/Aem.67.4.1893-1901.2001>.
- Braker, G., Matthies, D., Hannig, M., Brandt, F.B., Brenzinger, K., Grongroft, A., 2015. Impact of land use management and soil properties on denitrifier communities of Namibian Savannas. *Microb. Ecol.* 70 (4):981–992. <https://doi.org/10.1007/s00248-015-0623-6>.
- Carlson, R.E., 1977. Trophic state index for lakes. *Limnol. Oceanogr.* 22 (2), 361–369.
- Carpenter, S.R., Caraco, N.F., Correll, D.L., Howarth, R.W., Sharpley, A.N., Smith, V.H., 1998. Nonpoint pollution of surface waters with phosphorus and nitrogen. *Ecol. Appl.* 8 (3): 559–568. <https://doi.org/10.2307/2641247>.
- Chaffin, J.D., Bridgeman, T.B., Bade, D.L., Mobilian, C.N., 2014. Summer phytoplankton nutrient limitation in Maumee Bay of Lake Erie during high-flow and low-flow years. *J. Great Lakes Res.* 40 (3):524–531. <https://doi.org/10.1016/j.jglr.2014.04.009>.
- Chislock, M.F., Sharp, K.L., Wilson, A.E., 2014. *Cylindrospermopsis racibarskii* dominates under very low and high nitrogen-to-phosphorus ratios. *Water Res.* 49:207–214. <https://doi.org/10.1016/j.watres.2013.11.022>.
- Clevinger, C.C., Heath, R.T., Bade, D.L., 2014. Oxygen use by nitrification in the hypolimnion and sediments of Lake Erie. *J. Great Lakes Res.* 40 (1):202–207. <https://doi.org/10.1016/j.jglr.2013.09.015>.
- Cunha, R.W., Garcia, M.D.N., Albertoni, E.F., Palma-Silva, C., 2013. Water quality of a shallow lagoon in rural area in Southern Brazil. *Revista Brasileira De Engenharia Agrícola E Ambiental* 17 (7):770–779. <https://doi.org/10.1590/S1415-43662013000700012>.
- Degobbi, D., Homme-Maslovska, E., Orto, A.A., Donazzolo, R., Pavoni, B., 1986. The role of alkaline phosphatase in the sediments of Venice Lagoon on nutrient regeneration. *Estuar. Coast. Shelf Sci.* 22 (4):425–437. [https://doi.org/10.1016/0272-7714\(86\)90066-1](https://doi.org/10.1016/0272-7714(86)90066-1).
- Deslippe, J.R., Jamali, H., Jha, N., Saggat, S., 2014. Denitrifier community size, structure and activity along a gradient of pasture to riparian soils. *Soil Biol. Biochem.* 71:48–60. <https://doi.org/10.1016/j.soilbio.2014.01.007>.
- Ginger, L.J., Zimmer, K.D., Herwig, B.R., Hanson, M.A., Hobbs, W.O., Small, G.E., Cotner, J.B., 2017. Watershed versus within-lake drivers of nitrogen: phosphorus dynamics in shallow lakes. *Ecol. Appl.* <https://doi.org/10.1002/eap.1599>.
- Glibert, P.M., 1998. Interactions of top-down and bottom-up control in planktonic nitrogen cycling. *Hydrobiologia* 363, 1–12.
- Glibert, P.M., 2017. Eutrophication, harmful algae and biodiversity - challenging paradigms in a world of complex nutrient changes. *Mar. Pollut. Bull.* <https://doi.org/10.1016/j.marpolbul.2017.04.027>.
- Golterman, H.L., 1996. Fractionation of sediment phosphate with chelating compounds: a simplification, and comparison with other methods. *Hydrobiologia* 335 (1):87–95. <https://doi.org/10.1007/Bf00013687>.
- Gu, Y.F., Wang, Y.Y., Xiang, Q.J., Yu, X.M., Zhao, K., Zhang, X.P., Lindstorm, K., Hu, Y.F., Liu, S. Q., 2017. Implications of wetland degradation for the potential denitrifying activity and bacterial populations with *nirS* genes as found in a succession in Qinghai-Tibet plateau, China. *Eur. J. Soil Biol.* 80:19–26. <https://doi.org/10.1016/j.ejsobi.2017.03.005>.
- Han, J.H., Kim, B., Kim, C., An, K.G., 2014. Ecosystem health evaluation of agricultural reservoirs using multi-metric lentic ecosystem health assessment (LEHA) model. *Paddy Water Environ.* 12:S7–S18. <https://doi.org/10.1007/s10333-014-0444-0>.
- Holmroos, H., Hietanen, S., Niemisto, J., Horppila, J., 2012. Sediment resuspension and denitrification affect the nitrogen to phosphorus ratio of shallow lake waters. *Fundam. Appl. Limnol.* 80 (3):193–205. <https://doi.org/10.1127/1863-9135/2012/0223>.
- Hoppe, H.G., 1983. Significance of exoenzymatic activities in the ecology of brackish water: measurements by means of methylumbelliferyl-substrates. *Mar. Ecol. Prog. Ser.* 11, 299–308.
- Huang, L.D., Li, Z.X., Bai, X.L., Lo, R.Y., Wu, H.S., Wei, D.Y., Yu, L.J., 2016. Laboratory study of phosphorus retention and release by eutrophic lake sediments: modeling and implications for P release assessments. *Ecol. Eng.* 95:438–446. <https://doi.org/10.1016/j.ecoleng.2016.06.089>.
- Isles, P.D.F., Xu, Y.Y., Stockwell, J.D., Schroth, A.W., 2017. Climate-driven changes in energy and mass inputs systematically alter nutrient concentration and stoichiometry in deep and shallow regions of Lake Champlain. *Biogeochemistry* 133 (2):201–217. <https://doi.org/10.1007/s10533-017-0327-8>.
- Jha, P.K., Minagawa, M., 2013. Assessment of denitrification process in lower Ishikari river system, Japan. *Chemosphere* 93 (9):1726–1733. <https://doi.org/10.1016/j.chemosphere.2013.05.048>.
- Kim, O.S., Imhoff, J.F., Witzel, K.P., Junier, P., 2011. Distribution of denitrifying bacterial communities in the stratified water column and sediment-water interface in two freshwater lakes and the Baltic Sea. *Aquat. Ecol.* 45 (1):99–112. <https://doi.org/10.1007/s10452-010-9335-7>.
- Levy-Booth, D.J., Winder, R.S., 2010. Quantification of nitrogen reductase and nitrite reductase genes in soil of thinned and clear-cut Douglas-fir stands by using real-time PCR. *Appl. Environ. Microbiol.* 76 (21):7116–7125. <https://doi.org/10.1128/Aem.02188-09>.
- Li, H., Song, C.L., Cao, X.Y., Zhou, Y.Y., 2016. The phosphorus release pathways and their mechanisms driven by organic carbon and nitrogen in sediments of eutrophic shallow lakes. *Sci. Total Environ.* 572:280–288. <https://doi.org/10.1016/j.scitotenv.2016.07.221>.
- Liu, J.Z., Luo, X.X., Zhang, N.M., Wu, Y.H., 2016. Phosphorus released from sediment of Dianchi Lake and its effect on growth of *Microcystis aeruginosa*. *Environ. Sci. Pollut. Res.* 23 (16):16321–16328. <https://doi.org/10.1007/s11356-016-6816-9>.
- Liu, Y.Q., Cao, X.Y., Hui, L., Zhou, Z.J., Wang, S.Y., Wang, Z.C., Song, C.L., Zhou, Y.Y., 2017. Distribution of phosphorus-solubilizing bacteria in relation to fractionation and sorption behaviors of phosphorus in sediment of the three gorges reservoir. *Environ. Sci. Pollut. Res.* 24 (21):17679–17687. <https://doi.org/10.1007/s11356-017-9339-0>.
- Lurling, M., Mackay, E., Reizel, K., Spears, B.M., 2016. Editorial - a critical perspective on geo-engineering for eutrophication management in lakes. *Water Res.* 97:1–10. <https://doi.org/10.1016/j.watres.2016.03.035>.
- Muller, S., Mitrovic, S.M., Baldwin, D.S., 2016. Oxygen and dissolved organic carbon control release of N, P and Fe from the sediments of a shallow, polymeric lake. *J. Soils Sediments* 16 (3):1109–1120. <https://doi.org/10.1007/s11368-015-1298-9>.
- Myrstener, M., Jonsson, A., Bergström, A.K., 2016. The effects of temperature and resource availability on denitrification and relative N_2O production in boreal lake sediments. *J. Environ. Sci. (China)* 47 (9):82–90. <https://doi.org/10.1016/j.jes.2016.03.003>.
- Peng, G.T., Fan, Z.Q., Wang, X.R., Chen, C., 2016. Photosynthetic response to nitrogen source and different ratios of nitrogen and phosphorus in toxic cyanobacteria, *Microcystis aeruginosa* FACHB-905. *J. Limnol.* 75 (3):560–570. <https://doi.org/10.4081/jlimnol.2016.1458>.
- Sereda, J.M., Hudson, J.J., 2011. Empirical models for predicting the excretion of nutrients (N and P) by aquatic metazoans: taxonomic differences in rates and element ratios. *Freshw. Biol.* 56 (2):250–263. <https://doi.org/10.1111/j.1365-2427.2010.02491.x>.
- Small, G.E., Finlay, J.C., Mickay, R.M.L., Rozmarynowicz, M.J., Brovold, S., Bullerjahn, G.S., Spokas, K., Sterner, R.W., 2016. Large differences in potential denitrification and sediment microbial communities across the Laurentian great lakes. *Biogeochemistry* 128 (3):353–368. <https://doi.org/10.1007/s10533-016-0212-x>.
- Sondergaard, M., Lauridsen, T.L., Johansson, L.S., Jeppesen, E., 2017. Nitrogen or phosphorus limitation in lakes and its impact on phytoplankton biomass and submerged macrophyte cover. *Hydrobiologia* 795 (1):35–48. <https://doi.org/10.1007/s10750-017-3110-x>.
- Song, C.L., Cao, X.Y., Liu, Y.B., Zhou, Y.Y., 2009. Seasonal variations in chlorophyll *a* concentrations in relation to potentials of sediment phosphate release by different mechanisms in a large Chinese shallow eutrophic lake (Lake Taihu). *Geomicrobiol. J.* 26 (8):508–515. <https://doi.org/10.1080/01490450903061119>.
- Standard Methods for the Examination of Water and Wastewater 22nd ed. American Public Health Association, Washington, DC, USA.
- Tang, Y.C., Zhang, X.Y., Li, D.D., Wang, H.M., Chen, F.S., Fu, X.L., Fang, X.M., Sun, X.M., Yu, G. R., 2016. Impacts of nitrogen and phosphorus additions on the abundance and community structure of ammonia oxidizers and denitrifying bacteria in Chinese fir plantations. *Soil Biol. Biochem.* 103:284–293. <https://doi.org/10.1016/j.soilbio.2016.09.001>.
- Tatariw, C., Chapman, E.L., Sponseller, R.A., Mortazavi, B., Edmonds, J.W., 2013. Denitrification in a large river: consideration of geomorphic controls on microbial activity and community structure. *Ecology* 94 (10):2249–2262. <https://doi.org/10.1890/12-1765.1>.

- Ter Braak, C.J.F., Šmilauer, P., 2002. CANOCO Reference Manual and CanoDraw for Windows User's Guide: Software for Canonical Community Ordination (Version 4.5). Microcomputer Power, Ithaca, N.Y., USA.
- Vollenweider, R., 1992. Coastal marine eutrophication: principles and control. *Sci. Total Environ.* 126, 1–20 (suppl.).
- Wang, N., Ding, L.J., Xu, H.J., Li, H.B., Su, J.Q., Zhu, Y.G., 2015. Variability in responses of bacterial communities and nitrogen oxide emission to urea fertilization among various flooded paddy soils. *FEMS Microbiol. Ecol.* 91 (3). <https://doi.org/10.1093/femsec/fiv013>.
- Wang, F., Zhao, Y., Xie, S., Li, J., 2017. Implication of nitrifying and denitrifying bacteria for nitrogen removal in a shallow lake. *Clean: Soil, Air, Water* 45 (4). <https://doi.org/10.1002/clen.201500319>.
- Ward, B.B., 2013. How nitrogen is lost. *Science* 341 (6144), 352–353.
- Wu, Z., Liu, Y., Liang, Z., Wu, S., Guo, H., 2017. Internal cycling, not external loading, decides the nutrient limitation in eutrophic lake: a dynamic model with temporal Bayesian hierarchical inference. *Water Res.* 116:231–240. <https://doi.org/10.1016/j.watres.2017.03.039>.
- Yan, Z.B., Han, W.X., Penuelas, J., Sardans, J., Elser, J.J., Du, E.Z., Reich, P.B., Fang, J.Y., 2016. Phosphorus accumulates faster than nitrogen globally in freshwater ecosystems under anthropogenic impacts. *Ecol. Lett.* 19 (10):1237–1246. <https://doi.org/10.1111/ele.12658>.
- Yin, C., Fan, F.L., Song, A.L., Cui, P.Y., Li, T.Q., Liang, Y.C., 2015. Denitrification potential under different fertilization regimes is closely coupled with changes in the denitrifying community in a black soil. *Appl. Microbiol. Biotechnol.* 99 (13): 5719–5729. <https://doi.org/10.1007/s00253-015-6461-0>.
- Zehr, J.P., Ward, B.B., 2002. Nitrogen cycling in the ocean: new perspectives on processes and paradigms. *Appl. Environ. Microbiol.* 68 (3):1015–1024. <https://doi.org/10.1128/AEM.68.3.1015-1024.2002>.
- Zhou, S.L., Huang, T.L., Zhang, H.H., Zeng, M.Z., Liu, F., Bai, S.Y., Shi, J.C., Qiu, X.P., Yang, X., 2016. Nitrogen removal characteristics of enhanced in situ indigenous aerobic denitrification bacteria for micro-polluted reservoir source water. *Bioresour. Technol.* 201:195–207. <https://doi.org/10.1016/j.biortech.2015.11.041>.
- Zumft, W.G., 1997. Cell biology and molecular basis of denitrification. *Microbiol. Mol. Biol. Rev.* 61 (4), 533–616.